Plant Omics Journal POJ

POJ 7(5):308-321 (2014) ISSN:1836-3644

MicroRNA*s in apple (*Malus domestica*): biological implications obtained from high-throughput sequencing data

Chaogang Shao[1†], Xiaoxia Ma[2†], Guofu Lu[1], Yijun Meng[2*]

[1]College of Life Sciences, Huzhou Teachers College, Huzhou 313000, P. R. China
[2]College of Life and Environmental Sciences, Hangzhou Normal University, Hangzhou 310036, P. R. China

[†]These authors contributed equally to this work.

[*]Corresponding author: mengyijun@zju.edu.cn

Abstract

MicroRNAs (miRNAs) play important roles in diverse biological processes in plants through the regulation of gene expression. Recently, the plant miRNA* species have been uncovered to possess potential biological functions through target cleavages, which is similar to the miRNAs. By utilizing the publicly available small RNA high-throughput sequencing data, we performed a comprehensive search for the miRNA* sequences on the currently annotated miRNA precursors of apple. This search was based on the secondary structures of miRNA precursors and the accumulation levels of the miRNA* candidates. As a result, 188 miRNA*s were identified on 170 pre-miRNAs in apple. The organ-specific accumulation patterns of the identified miRNA*s were investigated. The result shows that some of the miRNA*s are highly abundant in the apple leaves, roots, flowers or fruits, indicating the potential organ-specific functions of these miRNA*s. Several pieces of literature-based hints were obtained to link the organ-specific accumulation patterns of the miRNA*s to their potential biological roles in organ development. To gain deeper insights into the biological roles of the miRNA*s in apple, degradome sequencing data-based target identification was performed. The result shows that certain miRNA*s possess great potential of performing target cleavage-based regulation of gene expression. Taken together, our study could advance the current understanding on the regulatory activities of the miRNA*s in the non-model plant apple tree.

Keywords: Apple (*Malus domestica*); degradome; high-throughput sequencing (HTS); microRNA*; organ-specific accumulation; target.
Abbreviations: miRNA_microRNA; HTS_high-throughput sequencing; pri-miRNA_primary microRNA; pre-miRNA_precursor microRNA; DCL1_Dicer-like 1; AGO_Argonaute; RISC_RNA-induced silencing complex; U_uridine; RPM_reads per million; GEO_Gene Expression Omnibus; GDR_Genome Database for Rosaceae.

Introduction

MicroRNAs (miRNAs) play essential regulatory roles in gene expression, which is involved in diverse biological processes in plants (Chen 2009; Jones-Rhoades et al., 2006). Most of the plant miRNA genes are transcribed by RNA polymerase II (Lee et al., 2004; Xie et al., 2005), resulting in poly(A)-tailed pri-miRNAs (primary microRNAs). The pri-miRNAs are processed to pre-miRNAs (precursor microRNAs), and then to ~21-bp miRNA:miRNA* duplexes by DCL1 (Dicer-like 1)-mediated two-step cleavages (Voinnet 2009). To exert regulatory role, the miRNA strand, also called the guide strand, of a short duplex is incorporated into a specific AGO (Argonaute)-associated RISC (RNA-induced silencing complex). A dominant portion of the plant miRNAs are 21 nt in length and start with 5' U (uridine). Thus, they are selectively recruited by AGO1-associated RISCs (Mi et al., 2008). Upon loading into the AGO1-associated RISC, the miRNA could guide the silencing complex to bind to a specific target transcripts based on a highly complementary recognition site, thus enabling subsequent cleavage-based regulation at the post-transcriptional level. The cleavage-based regulatory actions could be detected by a high-throughput method called degradome sequencing which allows us to map the slicing sites on the target transcripts by using degradome signatures (German et al., 2009; German et al., 2008). On the other hand, the miRNA* is subjected to rapid degradation due to the lack of the protection from the AGO protein complex (Jones-Rhoades et al., 2006; Voinnet 2009). Considering the much lower abundances of the star strands when compared to the mature miRNAs, the regulatory activities of the miRNA* species have been ignored for a long time. Until recently, a few studies uncovered the biological functions of the miRNA*s in plants including Arabidopsis (*Arabidopsis thaliana*), rice (*Oryza sativa*), soybean (*Glycine Max*) and *Medicago truncatula* (Devers et al., 2011; Manavella et al., 2013; Meng et al., 2011; Wong et al., 2011; Zhang et al., 2011). Based on sRNA high-throughput sequencing, a recent study by Xia et al. (2012) provide a global view of the organ-specific accumulation patterns of the apple (*Malus domestica*) miRNAs. By employing degradome sequencing technology, 118 target genes were identified (Xia et al., 2012). However, to our knowledge, the miRNA*s of *Malus domestica* have not been identified. No study has been carried out to investigate the organ-specific accumulation patterns and the potential regulatory activities of the miRNA*s in the non-model plant *Malus domestica*. Based on the valuable sequencing data provided by Xia et al. (2012), we did a systematic search for the miRNA*s of all the apple miRNA genes registered in miRBase (release 19) (Griffiths-Jones et al., 2008). As a result, 188 miRNA*s were

identified on 170 pre-miRNAs in apple. The organ-specific accumulation patterns of all the identified miRNA*s were investigated. Degradome sequencing data-based approach enabled us to identify dozens of target genes of the miRNA*s belonging to seven miRNA families. These results indicate that some of the apple miRNA*s are highly abundant in specific organs, and certain star sequences possess great potential of performing target cleavage-based regulation of gene expression. Taken together, this study could advance the current understanding on the regulatory activities of the miRNA*s in the non-model plant apple tree.

Results and Discussion

sRNA HTS data-based identification of miRNA*s in apple

A systematic search for the miRNA*s was performed in apple. Similar approach was employed by our previous study on the miRNA*s of Arabidopsis and rice (Shao et al., 2013). Specifically, a total of 206 pre-miRNA sequences were retrieved from miRBase (release 19) (Griffiths-Jones et al., 2008). Then, the short reads of four sRNA HTS data sets [GSM880652 (prepared from the apple leaves), GSM880653 (apple roots), GSM880654 (apple flowers) and GSM880655 (apple fruits)] were mapped to these pre-miRNAs by using an in-house Perl script, and only the perfect-match reads were retained for the following analyses (Data S1). Then, by using RNAshapes (Steffen et al., 2006), the secondary structures were predicted for all of the pre-miRNAs with perfect-match sRNA reads. Referring to the positions of the miRBase-registered miRNAs on the stem-loop structured pre-miRNAs, manual screening was carried out to extract the miRNA* candidates from the perfect-match reads. The screening was based on the two notions: (1) resulting from DCL1-mediated two-step cleavages, the miRNA:miRNA* duplex possesses 2-nt 3' overhangs at both ends (Jones-Rhoades et al., 2006; Voinnet, 2009); (2) previous studies showed that the abundances of the miRNA*s were much lower than the miRNA cognates (frequently one or more magnitudes lower), but much higher than the other sRNAs generated from the corresponding pre-miRNAs often by several magnitudes (Meng et al., 2011; Ruby et al., 2007). As a result, 188 miRNA*s were identified on 170 pre-miRNAs in apple (Fig 1, Fig S1 and Data S2). Among the 188 miRNA* candidates, most of them could pair with the miRNA cognates to form short duplexes with 2-nt 3' overhangs at both ends. Only a few miRNA:miRNA* duplexes identified on certain pre-miRNAs, such as mdm-MIR408b, mdm-MIR408d, mdm-MIR3627c, mdm-MIR7123a, mdm-MIR7123b and mdm-MIR7128 (Fig S1), have 1-nt or 3-nt 3' overhangs instead of 2-nt overhangs. It likely resulted from the wobble effect of DCL1-mediated cleavages during miRNA processing. Moreover, based on the relatively high abundances, two miRNA* candidates were identified on each of the 18 pre-miRNAs (mdm-MIR156ab/ac/u/v/w, mdm-MIR159a/b, mdm-MIR172b/c, mdm-MIR394a/b, mdm-MIR395a, mdm-MIR396a/b/c/d/e and mdm-MIR3627c). As mentioned above, the mature miRNA should be much more abundant than the miRNA*. And, the mature miRNAs belonging to the same family should share high sequence identity. Based on these two points, mdm-miR167a, mdm-miR393d, mdm-miR393e and mdm-miR393f currently registered as mature miRNAs in miRBase were corrected to be mdm-miR167a*, mdm-miR393d*, mdm-miR393e* and mdm-miR393f*, respectively. The corrected mature miRNAs were identified (see Data S1). The sequence characteristics of the 188 miRNA*s were analyzed, treating the 207 miRBase-registered miRNAs as a comparison. The result shows that the sequence length distributions are quite similar between the miRNA*s and the miRNAs. The 21-nt ones occupy the dominant portions (Fig 2A). However, difference was observed for the 5' terminal nucleotide compositions. A large portion of the miRNAs (143 out of 207) start with 5' U, whereas 101 out of 188 miRNA*s begin with 5' G (Fig 2B).

Degradome sequencing data-based evidences for the biogenesis of miRNAs and miRNA*s

Based on the previously proposed model, the slicing sites of DCL1 on the miRNA precursors during miRNA biogenesis could be mapped by using degradome sequencing (Meng et al., 2010). To validate the miRNA* candidates identified above, we set out to search for the degradome signatures that could be mapped onto either ends of the miRNA*s on the pre-miRNAs. The apple degradome sequencing data set (GSM880656) provided by Xia et al. (2012) was utilized for this analysis. All of the degradome signatures were mapped onto the 170 pre-miRNAs with identified miRNA*s, and only the perfect-match signatures were retained. As a result, 63 pre-miRNAs with perfect-match degradome signatures were retained (Data S3). After manual screening, 27 pre-miRNAs were identified to possess degradome signatures with 5' ends mapped to the 5' or the 3' ends of the mature miRNAs (Data S4), and four pre-miRNAs (mdm-MIR156o, mdm-MIR160c, mdm-MIR482c and mdm-MIR828a) were identified to possess degradome signatures with 5' ends mapped to the 5' ends of the miRNA*s (Fig 1). The relatively high frequency of the degradome signatures observed at the ends of the miRNAs might reflect the relatively high stability of the miRNA-containing remnants produced by DCL 1-mediated cleavages. On the other hand, limited degradome-based evidences were obtained for the processing of miRNA*s, which could result from the relatively low stability of the miRNA*-containing processing remnants and the limited degradome sequencing data available for this analysis.

Organ-specific accumulation patterns of the miRNA*s

The organ-specific accumulation patterns of the miRNA*s were investigated based on the four sRNA HTS data sets [GSM880652 (leaves), GSM880653 (roots), GSM880654 (flowers) and GSM880655 (fruits)] utilized in the above analysis. Organ-specific accumulation of a miRNA* was defined as following: the accumulation level of the miRNA* in a specific organ should occupy 50% or more of its total accumulation level in the four organs. As a result, dozens of miRNA*s were observed to accumulate with organ-specific patterns (Table 1 and Table 2). For examples, mdm-miR166a*/g*/h*, mdm-miR172e*, mdm-miR396c*-1 /d*-1/e*-1, mdm-miR399b*, mdm-miR399e*/f*, mdm-miR399g*/h*, and mdm-miR482b*/c* were highly accumulated in leaves when compared to the other three organs, and the accumulation levels of these miRNA*s in the leaf organ were more than 20 RPM (reads per million, see Materials and Methods for the calculation method). mdm-miR156g*/i*/o*, mdm-miR160a*/e*, mdm-miR408a* and mdm-miR447* were highly accumulated in roots with accumulation levels higher than 20 RPM. mdm-miR167a*/h*/i*/j*, mdm-miR172b*-2/o* and mdm-miR390a*/b*/e*/f* were highly accumulated in flowers with levels higher than 20 RPM. mdm-miR172d*/f*/i*/j*/k*/l* and mdm-miR7121d*/e*/g*/h* were highly accumulated in fruits with levels higher than 20 RPM. Among these organ-specific miRNA*s, some were found

Table 1. List of microRNA genes with consistent organ-specific accumulation patterns between the mature microRNAs and the microRNA*s. To show the organ-specific accumulation patterns of the microRNAs and microRNA*s, the accumulation levels (in RPM, reads per million) are highlighted in gray background.

miRNA/miRNA* ID	miRNA/miRNA* sequence	GSM880652 leaf	GSM880653 root	GSM880654 flower	GSM880655 fruit
mdm-miR166a/mdm-miR166b/mdm-miR166d/ mdm-miR166f/mdm-miR166g/mdm-miR166h	UCGGACCAGGCUUCAUUCCCC	13848.6	7382.09	196.46	283.82
mdm-miR166a*/mdm-miR166g*/mdm-miR166h*	GGAAUGUUGUCUGGCUCGAGG	183.89	108.1	0.18	1.18
mdm-miR166b*/mdm-miR166f*	GGAAUGCUGUCUGGUUCGAGA	0.08	0	0	0
mdm-miR166d*	GGAAUGUUGUUUGGCUCGAGG	7.91	3.55	0.37	0.22
mdm-miR172e	AGAAUCUUGAUGAUGCUGCAU	2186	65.03	548.57	186.67
mdm-miR172e*	GCCGCAUCACCAAGAUUCUUA	42.32	0	0	0
mdm-miR399e/mdm-miR399f/mdm-miR399g/ mdm-miR399h	UGCCAAAGGAGAUUUGCUCGG	1750.46	45.64	6.25	73.03
mdm-miR399e*/mdm-miR399f*	GGGCAAAGUCUCUUCUGGCAUG	60.32	0.19	0.18	4.42
mdm-miR399g*/mdm-miR399h*	GAGCAAAGUCUCCUCUGGCAUG	22.27	1.12	0	0.11
mdm-miR156d/mdm-miR156g/mdm-miR156i/ mdm-miR156l/mdm-miR156o	UGACAGAAGAGAGUGAGCAC	715.83	82324.33	306.54	25.85
mdm-miR156d*/mdm-miR156l*	GCUCACUUCUCUUUCUGUCAGC	0	0.24	0	0
mdm-miR156g*/mdm-miR156i*	GCUUAAUCUCUAUCUGUCGCC	0	149.31	0	0
mdm-miR156o*	GCUUACUCUCUAUCUGUCACC	0	29.11	0.55	0
mdm-miR160a/mdm-miR160b/mdm-miR160c/ mdm-miR160d/mdm-miR160e	UGCCUGGCUCCCUGUAUGCCA	6.2	29.94	14.7	6.68
mdm-miR160a*	GCGUACAAGGAGCCAAGCAUA	14.36	128.02	0	1.4
mdm-miR160b*/mdm-miR160d*	GCGUAUGAGGAGUCAAGCAUA	1.21	7.39	0.92	2.15
mdm-miR160c*	GCGUAUGAGGAGCCAAGCAUA	3.39	14.14	1.29	1.29
mdm-miR160e*	GCGUAUGAGGAGCCAUGCAUA	64.67	89.97	1.84	11.96
mdm-miR171m	UUGAGCCGUGCCAAUAUCACA	0.13	3.31	0.55	2.15
mdm-miR171m*	GGAUGUUGGAAUGGCUCAAUC	0.04	5.05	0	0
mdm-miR2111a/mdm-miR2111b	UAAUCUGCAUCCUGAGGUUUA	1.72	3.11	0.92	0
mdm-miR2111a*/mdm-miR2111b*	GUCCUUGGGAUGCAGAUUACC	0.04	0.53	0	0.43
mdm-miR397a/mdm-miR397b	UUGAGUGCAGCGUUGAUGAAA	1.55	52.64	0.37	0.65
mdm-miR397a*	UCGUCAGCUGUGCACCCAAUU	0	0.78	0	0
mdm-miR397b*	UCAUCAACGCUGCACCCAAUU	0	0.24	0	0
mdm-miR408a	AUGCACUGCCUCUUCCCUGGC	4.27	242.1	0	0
mdm-miR408a*	CAGGGAAGAGGUAGAGCAUGG	34.12	911.87	0.55	3.45
mdm-miR408b/mdm-miR408d	ACAGGGAAGAGGUAGAGCAUG	874.85	18196.45	0	9.16
mdm-miR408b*/mdm-miR408d*	UGCACUGCCUCUUCCCUGG	0.04	0.15	0	0
mdm-miR5225a/mdm-miR5225b	UCUGUCGAAGGUGAGAUGGUGC	7.7	49.72	0.55	0.22
mdm-miR5225a*/mdm-miR5225b*	UUCAUCCCUCCUCGACUGAAG	0.04	0.05	0	0
mdm-miR169a	CAGCCAAGGAUGACUUGCCGG	0.17	0.39	102.91	2.59
mdm-miR169a*	GGCAAGUUGCUCUUGGCUACA	0	0.05	1.29	0

mdm-miR169b	UAGCCAAGGAUGAUUUGCCUGC	0.04	0	3.12	0.32
mdm-miR169b*	AGGCAGUCACGCCUUGGCGACG	0	0	0.18	0
mdm-miR169c/mdm-miR169d	UAGCCAAGGAUGACUUGCCCG	0	0.05	2.21	1.29
mdm-miR169c*/mdm-miR169d*	GGCAGUCUCCUUGGCUAAU	0	0	0.37	0.32
mdm-miR171f	UUGAGCCGUGCCAAUAUCACG	1.42	0	12.13	0.75
mdm-miR171f*	GGAUAUUGGUCCGGUUCAAUA	0	0	16.36	1.51
mdm-miR172o	AGAAUCUUGAUGAUGCUGCAG	1.38	13.51	449.88	47.72
mdm-miR172o*	GGAGCAUCUUCAAGAUUCACA	0	0.53	21.5	4.95
mdm-miR390a/mdm-miR390b/mdm-miR390d/ mdm-miR390e/mdm-miR390f	AAGCUCAGGAGGGAUAGCGCC	7.2	15.65	278.24	2.59
mdm-miR390a*/mdm-miR390b*	CGCUAUCCAUCCUGAGUUUCA	2.85	0.44	159.7	1.51
mdm-miR390d*	GCUAUCCAUCCUGAGUUUCA	0	0	2.39	0.11
mdm-miR390e*/mdm-miR390f*	CGCUAUCCAUCUUGGGCUUCA	0.96	2.04	88.58	0.75
mdm-miR394a/mdm-miR394b	UUGGCAUUCUGUCCACCUCC	4.4	2.92	47.78	6.57
mdm-miR394a*-1/mdm-miR394b*-1	AGGUGGGCAUACUGCCAAC	0	0	0.18	0.11
mdm-miR394a*-2/mdm-miR394b*-2	AGGUGGGCAUACUGCCAACAG	0	0	0.55	0
mdm-miR395a/mdm-miR395c/mdm-miR395d/ mdm-miR395e/mdm-miR395f/mdm-miR395g/ mdm-miR395i	CUGAAGUGUUUGGGGGAACUC	23.44	3.4	241.11	53.21
mdm-miR395a*-2	GUUCCCCCGAAUACUUCAUUA	0.63	0.05	1.29	0.22
mdm-miR395c*/mdm-miR395e*/mdm-miR395f*	GUUCCCCCGAACACUUCAUUA	0	0	0.37	0.11
mdm-miR395d*/mdm-miR395g*/mdm-miR395i*	GUUCCCUUGACCACUUCAUUG	0.17	0	4.23	0.11
mdm-miR828a	UCUUGCUCAAAUGAGUAUUCCA	0	0.1	162.27	29.84
mdm-miR828a*	GAUGCUCAUUUGAGCAAGCAG	0	0	0.37	0
mdm-miR171i	UGAGCCGAACCAAUAUCACUC	2.18	0.87	17.09	73.25
mdm-miR171i*	GUGAUAUUGGUUUUGGCUCAUA	0	0	0.37	0.54
mdm-miR399a	UGCCAAAGGAGAAUUGCCCUG	87.9	1.07	88.03	253.88
mdm-miR399a*	GUGCAAUUCUCCUUUGGCAGA	4.73	0.24	5.15	10.99
mdm-miR7128	AUCAUUAACACUUAAUAACGA	0.04	0	0	1.51
mdm-miR7128*	UUAUUAAGUGUUAAUGAUUGG	0.08	0	0	0.11
mdm-miR858	UUCGUUGUCUGUUCGACCUGA	9.75	100.51	42.64	981.16
mdm-miR858*	AGGUCGAACAGACAGCGAACC	0	0	3.86	5.39

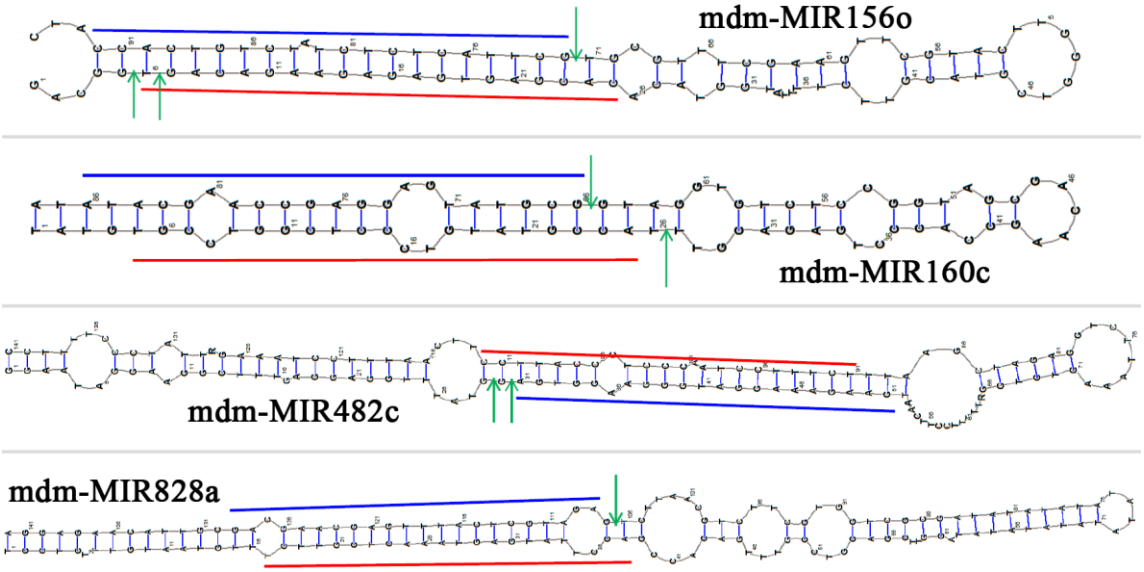

Fig 1. Examples of the identified microRNA*s (miRNA*s) and degradome sequencing data-based evidences for the biogenesis of the miRNA:miRNA* duplexes. The mature miRNAs (based on miRBase release 19) and the miRNA*s were denoted by red and blue lines on the pre-miRNAs (precursor microRNAs) respectively. The secondary structures of the pre-miRNAs were predicted by using RNAshapes (Steffen et al. 2006). Cleavage sites for the processing of the miRNA gene products were denoted by green arrows, which were supported by degradome signatures.

to share similar organ-specific accumulation patterns with their miRNA cognates (Table 1). For instances, both the mature miRNAs and the star sequences of miR166a/b/d/f/g/h, miR172e and miR399e/f/g/h were highly accumulated in the leaves. The mature miRNAs and the star sequences of miR156, miR160 and miR408 families were highly abundant in the roots. The mature miRNAs and the star sequences of miR390 family, miR171f and miR172o were highly accumulated in the flowers. The mature miRNAs and the star sequences of miR171i, miR399a and miR858 were highly abundant in the fruits (Table 1). The consistent organ-specific accumulation patterns between miRNAs and miRNA*s of specific families led us to propose that the star species might play redundant roles with the miRNA cognates in the development of specific organs of the apple trees. To partially address the hypothesis, we set out to find literature-based evidences to link the organ-specific accumulation patterns of the miRNA*s to their potential biological roles in organ development. Fortunately, several pieces of evidences were obtained. Both miR166 and miR166* were highly abundant in apple leaves. In Arabidopsis and soybean, miR166 was demonstrated to be implicated in the development of shoot apical meristem (Jung and Park, 2007; Wong et al., 2011). And, miR166 also plays a role in leaf flattening in Arabidopsis (Liu et al., 2011). miR172e and miR172e* were also highly accumulated in the apple leaves. Supportive evidences were found in tomato. A previous study based on miRNA profiling of tomato leaf curl New Delhi virus (tolcndv) infected tomato leaves indicated that deregulation of miR159 and miR172 might be linked with leaf curl disease (Naqvi et al., 2010). Based on the leaf-specific accumulation pattern of miR166 and miR172 in apple, the developmental roles of the two miRNAs might be highly conserved in the non-model plant *Malus domestica*. However, whether the leaf-specifically accumulated miR166* and miR172* are implicated in leaf development needs further experimental investigations. miR160 looks to be important for root cap formation and adventitious root development in Arabidopsis (Gutierrez et al., 2009; Wang et al., 2005). The high abundances of miR160a*/b*/c*/d*/e* in the apple roots, which are similar to their mature miR160 cognates, indicate their potential role in root development. In the roots of maize, miR408 shows high sensitivity to nitrate availability (Trevisan et al., 2012; Xu et al., 2011). The root-specific accumulation patterns of both mature miRNAs and miRNA*s of miR408 in apple indicate that miR408 and miR408* might cooperate together to be involved in nitrogen signaling in the root systems, which needs further validation. Our previous study on an auxin-resistant rice mutant with abnormal root phenotype showed that miR171 was intensively repressed in the root of the mutant, indicating the potential role of miR171 in regulating root system architecture in rice (Meng et al., 2009). In the roots of apple trees, miR171m along with miR171m*, miR171h*, miR171j*, miR171k* and miR171l* were highly accumulated. Thus, whether miR171 and miR171* are critical for root development in apple needs in-depth investigations. In the flowers of apple trees, miR169a/b/c/d along with the star sequences was highly accumulated. A previous report demonstrated that miR169 was essential for controlling floral organ identity in *Petunia hybrida* and *Antirrhinum majus* (Cartolano et al., 2007). Thus, it is interesting to study on the potential role of miR169 and miR169* in floral organ development in *Malus domestica*. In barley, over-expression of miR171 led to late flowering (Curaba et al., 2013). Interestingly, miR171f, miR171f*, miR171a* and miR171b* were observed to be highly abundant in the floral organ of apple tree. Based on this observation, we proposed that miR171 and miR171* might have an important role in controlling the flowering of apple trees. The biological role of miR172 in regulating flowering time and floral patterning has been validated to be highly conserved in Arabidopsis, maize, rice and barley (Aukerman and Sakai, 2003; Chen, 2004; Zhu and Helliwell, 2011; Zhu et al., 2009). The flower-specific accumulation patterns of miR172o, miR172o* and miR172b* suggest that the conserved role of miR172 family in floral organ development might be conserved in apple, and miR172* might be also involved in flowering process. Taken together, several pieces of literature-based evidences point to the potential roles of certain organ-specific miRNA*s in organ development. To gain further

Table 2 List of microRNA*s with organ-specific accumulation patterns which were not found for the corresponding mature microRNAs. To show the organ-specific accumulation patterns of the microRNA*s, the accumulation levels (in RPM, reads per million) are highlighted in gray background.

miRNA/miRNA* ID	miRNA/miRNA* sequence	GSM880652 leaf	GSM880653 root	GSM880654 flower	GSM880655 fruit
mdm-miR159a*-1	AGCUCCUUUUGAUUCAAAAG	0.04	0	0	0
mdm-miR171c*	UGUUGGCCCGGUUCACUCAGA	0.08	0	0	0
mdm-miR171e*	UGUUGGCCCGGUUUCACUCAGA	0.46	0	0	0.43
mdm-miR396f*/mdm-miR396g*	GUUCAAGAAAGCUGUGAAAAA	0.04	0	0	0
mdm-miR7127a*	UGACAAAUUGGAUGAGUAUUC	0.04	0	0	0
mdm-miR393a*/mdm-miR393b*/mdm-miR393c*/ mdm-miR393d*/mdm-miR393e*/mdm-miR393f*	AUCAUGCGAUCCCUUCGGACG	8.87	2.19	0	0
mdm-miR395a*-1	GUUCCCCCGAAUACUUCAUU	4.19	2.58	0.55	0.65
mdm-miR396a*-1/mdm-miR396b*-1	UUCAAUAAAGCUGUGGGAAG	18.04	6.9	0.74	1.29
mdm-miR396c*-1/mdm-miR396d*-1/mdm-miR396e*-1	CUCAAGAAAGCUGUGGGAGA	50.57	10.4	16.72	22.73
mdm-miR398a*	GGUGUGAAACUGAGAACACAAA	7.74	0	2.02	3.02
mdm-miR399b*	GUGCAAAUCUCCUUUGGCAGA	24.03	1.31	4.23	8.94
mdm-miR482b*	AAUGGAAGGGUAGGAAAGAAG	819.35	253.86	106.96	35.76
mdm-miR482c*	AGUGGAAGGGUAGGAAAGAAG	1123.25	545.69	14.52	16.26
mdm-miR171h*	UGUUGGAAUGGCUCAAUCAAA	0	0.63	0	0
mdm-miR3627c*-2	UUGCCAUCUCUCCUGUGACCA	0.04	0.05	0	0
mdm-miR171j*/mdm-miR171k*/mdm-miR171l*	CGAUGUUGGUGAGGUUCAAUC	0.25	1.41	0.18	0.22
mdm-miR447*	CGAAGACUUGGGGAGAGUGA	0.59	49.53	3.31	3.55
mdm-miR156w*-1	GCUCUCUUUUCUUCUGUCAUC	0.04	0	0.55	0.11
mdm-miR159b*-1	AGCUCCCUUUGAUUCAAAAG	0	0.05	0.18	0
mdm-miR164a*	CAUGUGCUCUACCUCUCCAGC	0	0	0.55	0.11
mdm-miR164c*	CACGUGCUCCCCCUCUCCAAC	0	0	0.55	0.54
mdm-miR164d*	CACGUGCUCCCCUUCUCCAAC	0	0	0.74	0.22
mdm-miR172b*-1	GAGCAUCUUCAAGAUUCACA	0	0	0.18	0
mdm-miR319a*	AGAGCUUUCUUUAGUCCAUUC	0	0.05	0.18	0
mdm-miR403a*	AGUUUGUGCGUGAAUCGAACC	0	0	0.74	0
mdm-miR403b*	AGUUUGUGCCUGAAUCAAACC	0.04	0	0.37	0
mdm-miR535d*	GUGCUCUUUCUUGUUGUCAUA	0.17	0.29	0.55	0
mdm-miR7122a*/mdm-miR7122b*	ACCGUGUUUUUCUGUAUAAAG	0.13	0.05	0.74	0
mdm-miR7123a*/mdm-miR7123b*	CUUUUACCUAUCCCAUUCUGU	0.04	0	0.18	0
mdm-miR156c*/mdm-miR156h*/mdm-miR156j*	GCUCACCUCUCUCUCUGUCAGC	0.13	0	6.25	2.69
mdm-miR156f*/mdm-miR156k*/mdm-miR156n*	GCUCAUGUCUCUUUCUGUCAGC	0.13	5.1	15.62	0.11
mdm-miR159b*-2	AGCUCCCUUUGAUUCAAAAGC	0.46	1.7	14.52	0.75
mdm-miR167a*/mdm-miR167h*/mdm-miR167i*/ mdm-miR167j*	AGAUCAUCUGGCAGUUUCACC	0.8	1.75	26.83	1.51
mdm-miR167b*	GGUCAUGCUCUGACAGCUUCACU	0	0.24	2.39	0.75
mdm-miR167c*/mdm-miR167d*/mdm-miR167g*	GAUCAUGUGGUAGCUUCACC	0	0.05	4.41	3.77
mdm-miR167f*	GAUCAUGUGGUCGCUUCACC	0	0	6.25	0
mdm-miR171a*/mdm-miR171b*	AGGUAUUGACGCGCCUCAAUU	0	0.24	1.65	0
mdm-miR172b*-2	GGAGCAUCUUCAAGAUUCACA	0	0.53	21.5	4.95
mdm-miR319b*	AGAGCUUUCUUCAGUCCACUC	0	0.39	2.76	0.65
mdm-miR7124a*/mdm-miR7124b*	AAUAAAGUUGAUAUUGGUGUG	1.59	3.35	7.9	0

mdm-miR156a*/mdm-miR156e*	GCUCACUUCUCUCUCCGUCAGC	0	0	0	0.22
mdm-miR156u*-2/mdm-miR156v*-2	GCUUUCUCUUCUUCUGUCAUCA	0	0.05	0	0.54
mdm-miR156w*-2	GCUCUCUUUUCUUCUGUCAUCA	0	0	0	0.32
mdm-miR167e*	GGUCAUGCUCUGACAGCCUCACU	0	0	0	0.32
mdm-miR169e*/mdm-miR169f*	UGACAGCCUCUUCUUCUCAUG	0.04	0	0.37	0.43
mdm-miR172c*-1	GAGCAUCAUCAAGAUUCACA	0	0	0	0.22
mdm-miR3627c*-1	GUUGCCAUCUCUCCUGUGACC	0.13	0.05	0	0.32
mdm-miR398b*	GGAGUGACCUGAGAUCACAUG	0	0.24	0	0.75
mdm-miR399i*/mdm-miR399j*	GGGCUCCUCCCUCUUGGCAGG	0.04	0	0	0.11
mdm-miR827*	UUUGUUGCUGGUCACCUAGUU	0	0	0	0.11
mdm-miR1511*	UGUGGUAUCAGGACUAUGUUA	6.57	3.06	2.39	12.6
mdm-miR156u*-1/mdm-miR156v*-1	GCUUUCUCUUCUUCUGUCAUC	0.46	1.26	0	5.82
mdm-miR166c*	GGAAUGUUGUCUGGUUCGAGA	0.13	0.15	0	1.51
mdm-miR171n*	GGAUGUUGGUAUGGUUCAAUC	0	0.92	0	1.29
mdm-miR172d*/mdm-miR172f*/mdm-miR172i*/ mdm-miR172j*/mdm-miR172k*/mdm-miR172l*	GCAGCAUCAUCAAGAUUCACA	0.42	0.1	2.57	23.91
mdm-miR2118a*	GGACUUAGUAGCUCGGUGAGA	0.08	0.34	0.18	2.37
mdm-miR535a*	GUGCCCUCUCUUGUUGUCAUU	0	0.05	0	2.15
mdm-miR7120a*/mdm-miR7120b*	ACAGUCUGACAAUAUAACGUG	0.63	0.58	1.47	4.42
mdm-miR7121a*	AGGGUGAUUAACAAAGGGAUG	0.84	0	0	6.25
mdm-miR7121c*	AGGGUGAUUACCAAGGUGAUG	0.08	0.1	0.55	2.15
mdm-miR7121d*/mdm-miR7121e*/mdm-miR7121g*/ mdm-miR7121h*	AGGGUGGUUACCAAUGGGAUG	3.64	18.13	0	22.94

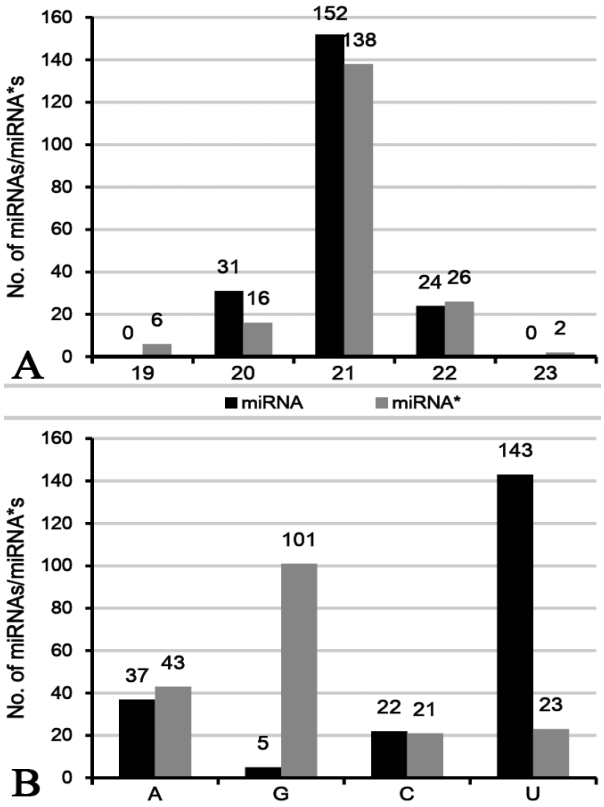

Fig 2. Sequence characteristics of the apple microRNA*s identified in this study. (A) Sequence length distribution. (B) 5' terminal nucleotide compositions. For (A) and (B), the mature miRNAs registered in miRBase (release 19) were included for comparison.

functional evidences of these miRNA*s, their target genes identified in this study (Table 3) could serve as a basis for in-depth experimental investigations. We also observed that some of the miRNA*s were accumulated in specific organs, while their miRNA cognates were not (Table 2). For examples, in the apple leaves, miR396a*-1, miR396b*-1, miR396c*-1, miR396d*-1, miR396e*-1, miR399b*, miR482b* and miR482c* were highly accumulated, while the corresponding miRNAs were not. Similarly, miR447* were abundant in the roots, miR156f*, miR156k*, miR156n*, miR159b*-2, miR167a*, miR167h*, miR167i* and miR172b*-2 were abundant in the flowers, and miR172d*, miR172f*, miR172i*, miR172j*, miR172k*, miR172l*, miR1511*, miR7121d*, miR7121e*, miR7121g* and miR7121h* were abundant in the apple fruits. Although we did not find direct evidences for the biological functions of these organ-specific miRNA*s, organ-specific regulatory roles of certain mature miRNAs were uncovered in the other plant species through literature mining, which correlated well with the organ-specific accumulation patterns of the corresponding miRNA*s in apple. miR159 controls leaf morphogenesis in Arabidopsis (Palatnik et al., 2003). Here, we observed that miR159a*-1 was exclusively detected in the leaves of apple trees, indicating its potential role in leaf development. miR393* was highly abundant in the apple leaves. A recent report in Arabidopsis showed that miR393 regulated the development of leaves through auxin signaling (Si-Ammour et al., 2011). miR396* was also highly abundant in the apple leaves. Notably, several studies demonstrated that miR396 was implicated in the growth and the development of leaf organ in Arabidopsis (Liu et al., 2009; Mecchia et al., 2012; Rodriguez et al., 2010; Wang et al., 2011). Certain star sequences of miR156 family were highly accumulated in the apple flowers. In Arabidopsis, it has been validated that miR156 plays an essential role in flowering (Wang et al., 2009; Xing et al., 2010; Yu et al., 2012). miR159b* was highly abundant in the apple flowers. In rice, miR159 regulates GAMYB in aleurone cells and anthers (Tsuji et al., 2006). miR164a*, miR164c* and miR164d* were specifically accumulated in the floral organ of apple tree. The role of miR164c in regulating petal number has been uncovered in Arabidopsis (Baker et al., 2005). miR167* possesses flower-specific accumulation pattern in apple. Accordingly, in Arabidopsis, miR167 involved in auxin signaling plays an essential role in reproduction (Nagpal et al., 2005; Ru et al., 2006; Wu et al., 2006). miR319a* and miR319b* were specifically enriched in the apple flowers. In Arabidopsis, miR319 is critical for petal growth and development, and flower maturation (Nag et al., 2009; Rubio-Somoza and Weigel, 2013). Several star sequences of miR156 family were specifically accumulated in the apple fruits. In tomato, miR156 was demonstrated to be involved in fruit development (Karlova et al., 2013; Zhang et al., 2011). miR172c*-1, miR172d*, miR172f*, miR172i*, miR172j*, miR172k* and miR172l* were highly abundant in the apple fruits. Based on a recent study by Karlova et al. (2013), miR172 shows great potential to be involved in tomato fruit development. All these functional hints point to a possibility that the organ-specific regulatory roles of certain miRNA genes discovered in the other plant species might be conserved in apple, but might be exerted by miRNA*s instead of the currently annotated mature miRNAs.

Degradome sequencing data-based identification of the miRNA* targets

As introduced above, most of the plant miRNAs exert their regulatory roles through target cleavages. Although both the organ-specific accumulation patterns and the literature-based functional hints were uncovered, whether the star species discovered in this study are capable of regulating specific target through cleavages are unclear. Here, by using degradome sequencing data set (GSM880656) provided by Xia et al. (2012), transcriptome-wide target prediction and validation were performed. First, all the miRNA*s identified in this study were included for target prediction by using miRU algorithm (Dai and Zhao, 2011; Zhang 2005). Referring to the previously proposed workflow (Meng et al., 2011), all the predicted targets were subjected to degradome sequencing data-based validation. As a result, four transcripts were validated to be targeted by miR156u*-1/v*-1, five transcripts were regulated by miR156u*-2/v*-2, five transcripts were targeted by miR159c*, two transcripts were regulated by miR166a*/e*/g*/h*/i*, one transcript MDP0000495468 was targeted by miR319c*, one transcript MDP0000129321 was targeted by miR396a*-1/a*-2/b*-1/b*-2, 29 transcripts were targeted by mdm-miR482d*, and two transcripts were regulated by miR7127a* (Table 3). These transcripts are reliable targets of the miRNA*s since most of the degradome signature-supported cleavage sites resided in the middle of the miRNA* binding sites (Fig 3 and Fig S2), which was regarded as the canonical feature of miRNA-guided target cleavages in plants (Jones-Rhoades et al., 2006; Voinnet, 2009). Next, we set out to investigate the potential functions of the above identified miRNA*--target pairs based on the annotations of the target transcripts. Interestingly, we observed that all the 29 transcripts targeted by miR482d* encode disease resistance proteins. Additionally, MDP0000267764 regulated by miR159c* encodes a TIR-NBS-LRR type disease resistance protein (Table 3). It implies that miR159c* and miR482d* might have

Table 3. List of the transcripts targeted by microRNA*s in apple (*Malus domestica*).

miRNA*	Target transcript	Target transcript annotation			
		BLAST-based annotation	Gene Ontology	KEGG pathway	KEGG ortholog
mdm-miR156u*-1/v*-1; mdm-miR156u*-2/v*-2	MDP0000244658	-	-	-	-
	MDP0000144208	-	-		
	MDP0000276544	-	GO:0003676 (nucleic acid binding)		
	MDP0000545009	-	-		
mdm-miR156u*-2/v*-2	MDP0000166757	OBERON 4-like	-		
mdm-miR159c*	MDP0000132983	Ubiquitin-conjugating enzyme E2 24-like	GO:0016881 (acid-amino acid ligase activity)		
	MDP0000483412	-	-		
	MDP0000848219	zinc finger CCCH domain-containing protein 41-like	GO:0003676 (nucleic acid binding); GO:0008270 (zinc ion binding)		
	MDP0000952010	-	-		
	MDP0000267764	TIR-NBS-LRR type disease resistance protein	GO:0005515 (protein binding); GO:0005622 (intracellular); GO:0006952 (defense response); GO:0007165 (signal transduction); GO:0043531 (ADP binding)		
mdm-miR166a*/h*/g*; mdm-miR166e*/i*	MDP0000271818	-	GO:0003676 (nucleic acid binding); GO:0009055 (electron carrier activity); GO:0015035 (protein disulfide oxidoreductase activity); GO:0045454 (cell redox homeostasis)		
	MDP0000288921	-	GO:0003676 (nucleic acid binding); GO:0009055 (electron carrier activity); GO:0015035 (protein disulfide oxidoreductase activity); GO:0045454 (cell redox homeostasis)		
mdm-miR319c*	MDP0000495468	LONGIFOLIA 1-like	-		
mdm-miR396a*-1/b*-1; mdm-miR396a*-2/b*-2	MDP0000129321	SC35-like splicing factor	GO:0000166 (nucleotide binding); GO:0003676 (nucleic acid binding)	ko03040 (Spliceosome); ko05168 (Herpes simplex infection)	K12891 (splicing factor, arginine/serine-rich 2)
mdm-miR482d*	MDP0000160232	disease resistance protein RGA3-like	GO:0005515 (protein binding); GO:0006952 (defense response); GO:0043531 (ADP binding)	-	-
	MDP0000166800	putative disease resistance protein RGA3-like	GO:0006952 (defense response); GO:0043531 (ADP binding)		
	MDP0000167895	disease resistance protein RGA3-like	GO:0005515 (protein binding); GO:0006952 (defense response); GO:0043531 (ADP binding)		
	MDP0000233739	disease resistance protein RGA3-like	GO:0005515 (protein binding); GO:0006952 (defense response); GO:0043531 (ADP binding)		
	MDP0000263446	disease resistance protein RGA3-like	GO:0005515 (protein binding); GO:0006952 (defense response); GO:0008219 (cell death); GO:0016021 (integral to membrane); GO:0043531 (ADP binding)		
	MDP0000285888	disease resistance protein RGA3-like	GO:0003723 (RNA binding); GO:0006952 (defense response); GO:0043531 (ADP binding)		
	MDP0000304601	disease resistance protein RGA3-like	GO:0005515 (protein binding); GO:0006952 (defense response); GO:0043531 (ADP binding)		
	MDP0000304705	disease resistance protein RGA1-like	GO:0006952 (defense response); GO:0043531 (ADP binding)		
	MDP0000309995	disease resistance protein RGA3-like	GO:0005515 (protein binding); GO:0006952 (defense response); GO:0043531 (ADP binding)		
	MDP0000312668	disease resistance protein RGA3-like	GO:0005515 (protein binding); GO:0006952 (defense response); GO:0043531 (ADP binding)		

	MDP0000316884	disease resistance protein RGA3-like	GO:0005515 (protein binding); GO:0006952 (defense response); GO:0043531 (ADP binding)		
	MDP0000336256	disease resistance protein RGA3-like	-		
	MDP0000367358	-	-		
	MDP0000415930	disease resistance protein RGA3-like	GO:0005515 (protein binding); GO:0006952 (defense response); GO:0043531 (ADP binding)		
	MDP0000464475	disease resistance protein RGA4-like	GO:0005515 (protein binding); GO:0043531 (ADP binding)		
	MDP0000704323	disease resistance protein RGA3-like	GO:0005515 (protein binding); GO:0006952 (defense response); GO:0043531 (ADP binding)		
	MDP0000775297	disease resistance protein RGA3-like	GO:0043531 (ADP binding)		
	MDP0000810351	disease resistance protein RGA3-like	GO:0005515 (protein binding); GO:0006952 (defense response); GO:0043531 (ADP binding)		
	MDP0000211316	disease resistance protein RGA3-like	GO:0005515 (protein binding); GO:0006952 (defense response); GO:0043531 (ADP binding)		
	MDP0000217718	disease resistance protein RGA3-like	GO:0043531 (ADP binding)		
	MDP0000248321	disease resistance protein RGA4-like	GO:0043531 (ADP binding)		
	MDP0000256429	disease resistance protein RGA3-like	GO:0005515 (protein binding); GO:0043531 (ADP binding)		
	MDP0000266073	disease resistance protein RGA3-like	GO:0000166 (nucleotide binding); GO:0003824 (catalytic activity); GO:0005515 (protein binding); GO:0006952 (defense response); GO:0043531 (ADP binding); GO:0044237 (cellular metabolic process); GO:0050662 (coenzyme binding)		
	MDP0000266458	disease resistance protein RGA3-like	GO:0006952 (defense response); GO:0043531 (ADP binding)		
	MDP0000272830	disease resistance protein RGA3-like	GO:0004672 (protein kinase activity); GO:0004713 (protein tyrosine kinase activity); GO:0005515 (protein binding); GO:0005524 (ATP binding); GO:0006468 (protein phosphorylation); GO:0006952 (defense response); GO:0016772 (transferase activity, transferring phosphorus-containing groups); GO:0043531 (ADP binding)		
	MDP0000275398	disease resistance protein RGA4-like	GO:0005515 (protein binding); GO:0006952 (defense response); GO:0043531 (ADP binding)		
	MDP0000287465	pentatricopeptide repeat (PPR)-containing protein	GO:0016740 (transferase activity); GO:0043531 (ADP binding)		
	MDP0000299465	disease resistance protein RGA3-like	GO:0005515 (protein binding); GO:0006952 (defense response); GO:0043531 (ADP binding)		
	MDP0000308635	disease resistance protein RGA3-like	GO:0006952 (defense response); GO:0043531 (ADP binding)		
mdm-miR7127a*	MDP0000302491	-	GO:0005515 (protein binding); GO:0008270 (zinc ion binding)		
	MDP0000350960	-	GO:0005515 (protein binding); GO:0008270 (zinc ion binding)		

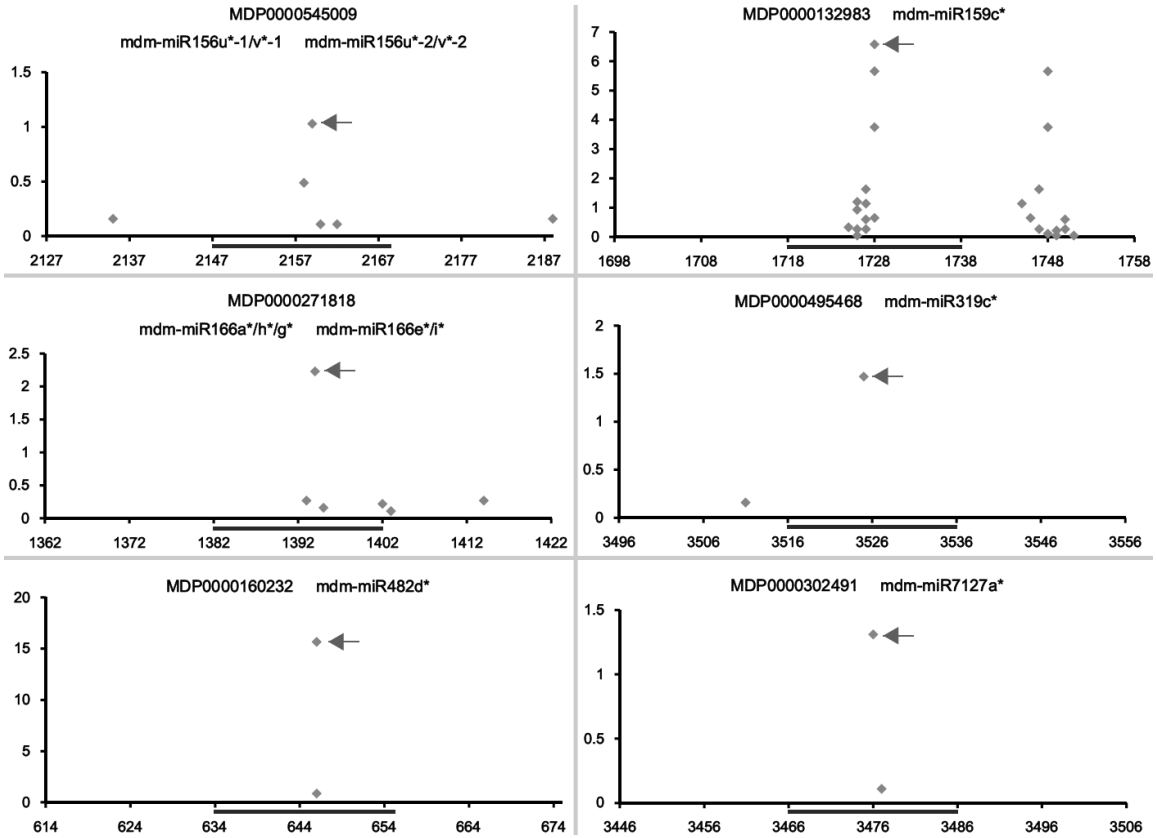

Fig 3. Degradome sequencing data-based validation of the targets regulated by the microRNA*s (miRNA*s) in apple. For all the figure panels, the IDs of the target transcripts and the miRNA*s are listed on the top. The *Y* axes measure the intensity (in RPM, reads per million) of the degradome signals, and the *X* axes indicate the positions of the cleavage signals on the target transcripts. The binding sites of the miRNA*s on their target transcripts were denoted by gray horizontal lines, and the dominant cleavage signals were marked by gray arrowheads.

biological roles in biotic stress response of apple trees. However, this hypothesis needs experimental verification. Besides, miR159c* targets another transcript MDP0000132983 encoding a ubiquitin-conjugating enzyme, suggesting its involvement in protein metabolism. MDP0000129321 encoding an SC35-like splicing factor was targeted by miR396a*-1, miR396b*-1, miR396a*-2 and miR396b*-2. Thus, it remains to be elucidated whether miR396* participates in messenger RNA processing. miR156u*-2 and miR156v*-2 target MDP0000166757 encoding an OBERON 4-like protein. In Arabidopsis, *OBERON1* and *OBERON2* encoding homeodomain finger proteins are required for the maintenance of both the shoot and the root meristems (Saiga et al., 2008), indicating the potential involvement of miR156* in meristem maintenance in apple trees. Interestingly, previous studies demonstrated that miR156 were important for meristem establishment and/or maintenance in Arabidopsis, rice and maize (Chuck et al., 2010; Luo et al., 2006; Wang et al., 2008). Thus, whether miR156* plays a similar role in apple needs experimental validation. miR319c* regulates MDP0000495468 encoding a LONGIFOLIA 1-like protein. In Arabidopsis, LONGIFOLIA1 and LONGIFOLIA2 regulate leaf morphology by positively promoting longitudinal polar cell elongation (Lee et al., 2006). Besides, in both tomato and rice, miR319 is required for leaf patterning (Ori et al., 2007; Shleizer-Burko et al., 2011; Yang et al., 2013). Thus, the potential role of miR319c* in apple leaf development uncovered in this study leaves to be further investigated.

Materials and Methods

Data sources

The sRNA HTS data and the degradome sequencing data of apple were the gift of a previous report by Xia et al. (2012), and were retrieved from GEO (Gene Expression Omnibus; http://www.ncbi.nlm.nih.gov/geo/) (Barrett et al., 2009) under accession ID GSE36065 [sRNA HTS data: GSM880652 (leaf), GSM880653 (root), GSM880654 (flower) and GSM880655 (fruit); degradome sequencing data: GSM880656 (mixed tissue)]. The miRNA sequences of apple were obtained from miRBase (release 19; http://www.mirbase.org/) (Griffiths-Jones et al., 2008). The apple transcripts along with the annotations were retrieved from the Genome Database for Rosaceae (GDR; http://www.rosaceae.org/species/malus/malus_x_domestica/genome_v1.0) (Jung et al., 2008).

Prediction and validation of the miRNA targets*

Target prediction was performed by using miRU algorithm (Dai and Zhao, 2011; Zhang, 2005) with default parameters. The degradome sequencing data were utilized to validate the predicted miRNA*—target pairs. First, in order to allow cross-library comparison, the normalized read count (in RPM, reads per million) of a short sequence from a specific degradome library was calculated by dividing the raw count of this sequence by the total counts of the library, and then multiplied by 10^6. Then, two-step filtering was performed to

extract the most likely miRNA*—target pairs. During the first step, the predicted miRNA* binding sites along with the 50-nt surrounding sequences at both ends were collected in order to reduce the BLAST time. The predicted targets met the following criterion were retained: there must be perfectly matched degradome signatures with their 5' ends resided within 8^{th} to 12^{th} nt region from the 5' ends of the miRNA*s. These retained transcripts were subjected to a second BLAST, and the degradome signals along each transcript were obtained to provide a global view of the signal noise when compared to the signal intensity within a specific target binding site. Referring to our previous study (Meng et al., 2011), both global and local t-plots were drawn. Finally, exhaustive manual filtering was performed, and only the transcripts with cleavage signals easy to be recognized were extracted as the miRNA*—target pairs.

Conclusions

Taken together, the miRNA*s identified in this study, the organ-specific accumulation patterns of certain miRNA*s, and the miRNA*--target pairs could advance our current understanding of the regulatory roles of miRNA*s in apple trees, and could serve as the basis for in-depth analysis of the miRNA gene-involved regulatory modules for organ development of apple trees.

Acknowledgments

The authors would like to thank all the publicly available datasets and the scientists behind them. This work was funded by the National Natural Science Foundation of China [31100937] and [31271380], the Starting Grant funded by Hangzhou Normal University to Yijun Meng [2011QDL60], and the Research Fund of Huzhou Teachers College [2013040].

References

Aukerman MJ, Sakai H (2003) Regulation of flowering time and floral organ identity by a microRNA and its APETALA2-like target genes. Plant Cell. 15:2730-2741.

Baker CC, Sieber P, Wellmer F, Meyerowitz EM (2005) The early extra petals1 mutant uncovers a role for microRNA miR164c in regulating petal number in Arabidopsis. Curr Biol. 15:303-315.

Barrett T, Troup DB, Wilhite SE, Ledoux P, Rudnev D, Evangelista C, Kim IF, Soboleva A, Tomashevsky M, Marshall KA, Phillippy KH, Sherman PM, Muertter RN, Edgar R (2009) NCBI GEO: archive for high-throughput functional genomic data. Nucleic Acids Res. 37:D885-890.

Cartolano M, Castillo R, Efremova N, Kuckenberg M, Zethof J, Gerats T, Schwarz-Sommer Z, Vandenbussche M (2007) A conserved microRNA module exerts homeotic control over *Petunia hybrida* and *Antirrhinum majus* floral organ identity. Nat Genet. 39:901-905.

Chen X (2004) A microRNA as a translational repressor of APETALA2 in Arabidopsis flower development. Science. 303:2022-2025.

Chen X (2009) Small RNAs and their roles in plant development. Annu Rev Cell Dev Biol. 25:21-44.

Chuck G, Whipple C, Jackson D, Hake S (2010) The maize SBP-box transcription factor encoded by tasselsheath4 regulates bract development and the establishment of meristem boundaries. Development. 137:1243-1250.

Curaba J, Talbot M, Li Z, Helliwell C (2013) Over-expression of microRNA171 affects phase transitions and floral meristem determinancy in barley. BMC Plant Biol. 13:6.

Dai X, Zhao PX (2011) psRNATarget: a plant small RNA target analysis server. Nucleic Acids Res. 39:W155-159.

Devers EA, Branscheid A, May P, Krajinski F (2011) Stars and symbiosis: microRNA- and microRNA*-mediated transcript cleavage involved in arbuscular mycorrhizal symbiosis. Plant Physiol. 156:1990-2010.

German MA, Luo S, Schroth G, Meyers BC, Green PJ (2009) Construction of parallel analysis of RNA ends (PARE) libraries for the study of cleaved miRNA targets and the RNA degradome. Nat Protoc. 4:356-362.

German MA, Pillay M, Jeong DH, Hetawal A, Luo S, Janardhanan P, Kannan V, Rymarquis LA, Nobuta K, German R, De Paoli E, Lu C, Schroth G, Meyers BC, Green PJ (2008) Global identification of microRNA-target RNA pairs by parallel analysis of RNA ends. Nat Biotechnol. 26:941-946.

Griffiths-Jones S, Saini HK, van Dongen S, Enright AJ (2008) miRBase: tools for microRNA genomics. Nucleic Acids Res. 36:D154-158.

Gutierrez L, Bussell JD, Pacurar DI, Schwambach J, Pacurar M, Bellini C (2009) Phenotypic plasticity of adventitious rooting in Arabidopsis is controlled by complex regulation of AUXIN RESPONSE FACTOR transcripts and microRNA abundance. Plant Cell. 21:3119-3132.

Jones-Rhoades MW, Bartel DP, Bartel B (2006) MicroRNAs and their regulatory roles in plants. Annu Rev Plant Biol. 57:19-53.

Jung JH, Park CM (2007) MIR166/165 genes exhibit dynamic expression patterns in regulating shoot apical meristem and floral development in Arabidopsis. Planta. 225:1327-1338.

Jung S, Staton M, Lee T, Blenda A, Svancara R, Abbott A, Main D (2008) GDR (Genome Database for Rosaceae): integrated web-database for Rosaceae genomics and genetics data. Nucleic Acids Res. 36:D1034-1040.

Karlova R, van Haarst JC, Maliepaard C, van de Geest H, Bovy AG, Lammers M, Angenent GC, de Maagd RA (2013) Identification of microRNA targets in tomato fruit development using high-throughput sequencing and degradome analysis. J Exp Bot. 64:1863-1878.

Lee Y, Kim M, Han J, Yeom KH, Lee S, Baek SH, Kim VN (2004) MicroRNA genes are transcribed by RNA polymerase II. EMBO J. 23:4051-4060.

Lee YK, Kim GT, Kim IJ, Park J, Kwak SS, Choi G, Chung WI (2006) LONGIFOLIA1 and LONGIFOLIA2, two homologous genes, regulate longitudinal cell elongation in Arabidopsis. Development. 133:4305-4314.

Liu D, Song Y, Chen Z, Yu D (2009) Ectopic expression of miR396 suppresses GRF target gene expression and alters leaf growth in Arabidopsis. Physiol Plant. 136:223-236.

Liu Z, Jia L, Wang H, He Y (2011) HYL1 regulates the balance between adaxial and abaxial identity for leaf flattening via miRNA-mediated pathways. J Exp Bot. 62:4367-4381.

Luo YC, Zhou H, Li Y, Chen JY, Yang JH, Chen YQ, Qu LH (2006) Rice embryogenic calli express a unique set of microRNAs, suggesting regulatory roles of microRNAs in plant post-embryogenic development. FEBS Lett. 580:5111-5116.

Manavella PA, Koenig D, Rubio-Somoza I, Burbano HA, Becker C, Weigel D (2013) Tissue-specific silencing of Arabidopsis SU(VAR)3-9 HOMOLOG8 by miR171a. Plant Physiol. 161:805-12.

Mecchia MA, Debernardi JM, Rodriguez RE, Schommer C, Palatnik JF (2012) MicroRNA miR396 and RDR6 synergistically regulate leaf development. Mech Dev. 130:2-13.

Meng Y, Gou L, Chen D, Wu P, Chen M (2010) High-throughput degradome sequencing can be used to gain insights into microRNA precursor metabolism. J Exp Bot. 61:3833-3837.

Meng Y, Huang F, Shi Q, Cao J, Chen D, Zhang J, Ni J, Wu P, Chen M (2009) Genome-wide survey of rice microRNAs and microRNA-target pairs in the root of a novel auxin-resistant mutant. Planta. 230:883-898.

Meng Y, Shao C, Chen M (2011) Toward microRNA-mediated gene regulatory networks in plants. Brief Bioinform. 12:645-659.

Meng Y, Shao C, Gou L, Jin Y, Chen M (2011) Construction of microRNA- and microRNA*-mediated regulatory networks in plants. RNA Biol. 8:1124-1148.

Mi S, Cai T, Hu Y, Chen Y, Hodges E, Ni F, Wu L, Li S, Zhou H, Long C, Chen S, Hannon GJ, Qi Y (2008) Sorting of small RNAs into Arabidopsis argonaute complexes is directed by the 5' terminal nucleotide. Cell. 133:116-127.

Nag A, King S, Jack T (2009) miR319a targeting of TCP4 is critical for petal growth and development in Arabidopsis. Proc Natl Acad Sci U S A. 106:22534-22539.

Nagpal P, Ellis CM, Weber H, Ploense SE, Barkawi LS, Guilfoyle TJ, Hagen G, Alonso JM, Cohen JD, Farmer EE, Ecker JR, Reed JW (2005) Auxin response factors ARF6 and ARF8 promote jasmonic acid production and flower maturation. Development. 132:4107-4118.

Naqvi AR, Haq QM, Mukherjee SK (2010) MicroRNA profiling of tomato leaf curl New Delhi virus (tolcndv) infected tomato leaves indicates that deregulation of mir159/319 and mir172 might be linked with leaf curl disease. Virol J. 7:281.

Ori N, Cohen AR, Etzioni A, Brand A, Yanai O, Shleizer S, Menda N, Amsellem Z, Efroni I, Pekker I, Alvarez JP, Blum E, Zamir D, Eshed Y (2007) Regulation of LANCEOLATE by miR319 is required for compound-leaf development in tomato. Nat Genet. 39:787-791.

Palatnik JF, Allen E, Wu X, Schommer C, Schwab R, Carrington JC, Weigel D (2003) Control of leaf morphogenesis by microRNAs. Nature. 425:257-263.

Rodriguez RE, Mecchia MA, Debernardi JM, Schommer C, Weigel D, Palatnik JF (2010) Control of cell proliferation in *Arabidopsis thaliana* by microRNA miR396. Development. 137:103-112.

Ru P, Xu L, Ma H, Huang H (2006) Plant fertility defects induced by the enhanced expression of microRNA167. Cell Res. 16:457-465.

Rubio-Somoza I, Weigel D (2013) Coordination of flower maturation by a regulatory circuit of three microRNAs. PLoS Genet. 9:e1003374.

Ruby JG, Stark A, Johnston WK, Kellis M, Bartel DP, Lai EC (2007) Evolution, biogenesis, expression, and target predictions of a substantially expanded set of Drosophila microRNAs. Genome Res. 17:1850-1864.

Saiga S, Furumizu C, Yokoyama R, Kurata T, Sato S, Kato T, Tabata S, Suzuki M, Komeda Y (2008) The Arabidopsis OBERON1 and OBERON2 genes encode plant homeodomain finger proteins and are required for apical meristem maintenance. Development. 135:1751-1759.

Shao C, Ma X, Xu X, Meng Y (2013) Identification of the highly accumulated microRNA*s in Arabidopsis (*Arabidopsis thaliana*) and rice (*Oryza sativa*). Gene. 515:123-127.

Shleizer-Burko S, Burko Y, Ben-Herzel O, Ori N (2011) Dynamic growth program regulated by LANCEOLATE enables flexible leaf patterning. Development. 138:695-704.

Si-Ammour A, Windels D, Arn-Bouldoires E, Kutter C, Ailhas J, Meins F, Vazquez F (2011) miR393 and secondary siRNAs regulate expression of the TIR1/AFB2 auxin receptor clade and auxin-related development of Arabidopsis leaves. Plant Physiol. 157:683-691.

Steffen P, Voss B, Rehmsmeier M, Reeder J, Giegerich R (2006) RNAshapes: an integrated RNA analysis package based on abstract shapes. Bioinformatics. 22:500-503.

Trevisan S, Nonis A, Begheldo M, Manoli A, Palme K, Caporale G, Ruperti B, Quaggiotti S (2012) Expression and tissue-specific localization of nitrate-responsive miRNAs in roots of maize seedlings. Plant Cell Environ. 35:1137-1155.

Tsuji H, Aya K, Ueguchi-Tanaka M, Shimada Y, Nakazono M, Watanabe R, Nishizawa NK, Gomi K, Shimada A, Kitano H, Ashikari M, Matsuoka M (2006) GAMYB controls different sets of genes and is differentially regulated by microRNA in aleurone cells and anthers. Plant J. 47:427-444.

Voinnet O (2009) Origin, biogenesis, and activity of plant microRNAs. Cell. 136:669-687.

Wang JW, Czech B, Weigel D (2009) miR156-regulated SPL transcription factors define an endogenous flowering pathway in *Arabidopsis thaliana*. Cell. 138:738-749.

Wang JW, R Schwab, B Czech, E Mica, D Weigel (2008) Dual effects of miR156-targeted SPL genes and CYP78A5/KLUH on plastochron length and organ size in *Arabidopsis thaliana*. Plant Cell. 20:1231-1243.

Wang JW, Wang LJ, Mao YB, Cai WJ, Xue HW, Chen XY (2005) Control of root cap formation by microRNA-targeted auxin response factors in Arabidopsis. Plant Cell. 17:2204-2216.

Wang L, Gu X, Xu D, Wang W, Wang H, Zeng M, Chang Z, Huang H, Cui X (2011) miR396-targeted AtGRF transcription factors are required for coordination of cell division and differentiation during leaf development in Arabidopsis. J Exp Bot. 62:761-773.

Wong CE, Zhao YT, Wang XJ, Croft L, Wang ZH, Haerizadeh F, Mattick JS, Singh MB, Carroll BJ, Bhalla PL (2011) MicroRNAs in the shoot apical meristem of soybean. J Exp Bot. 62:2495-2506.

Wu MF, Tian Q, Reed JW (2006) Arabidopsis microRNA167 controls patterns of ARF6 and ARF8 expression, and regulates both female and male reproduction. Development. 133:4211-4218.

Xia R, Zhu H, An YQ, Beers EP, Liu Z (2012) Apple miRNAs and tasiRNAs with novel regulatory networks. Genome Biol. 13:R47.

Xie Z, Allen E, Fahlgren N, Calamar A, Givan SA, Carrington JC (2005) Expression of Arabidopsis miRNA genes. Plant Physiol. 138:2145-2154.

Xing S, Salinas M, Hohmann S, Berndtgen R, Huijser P (2010) miR156-targeted and nontargeted SBP-box transcription factors act in concert to secure male fertility in Arabidopsis. Plant Cell. 22:3935-3950.

Xu Z, Zhong S, Li X, Li W, Rothstein SJ, Zhang S, Bi Y, Xie C (2011) Genome-wide identification of microRNAs in response to low nitrate availability in maize leaves and roots. PLoS One. 6:e28009.

Yang C, Li D, Mao D, Liu X, Ji C, Li X, Zhao X, Cheng Z, Chen C, Zhu L (2013) Overexpression of microRNA319 impacts leaf morphogenesis and leads to enhanced cold tolerance in rice (*Oryza sativa* L.). Plant Cell Environ. 36:2207-2218.

Yu S, Galvao VC, Zhang YC, Horrer D, Zhang TQ, Hao YH, Feng YQ, Wang S, Schmid M, Wang JW. (2012) Gibberellin regulates the Arabidopsis floral transition through miR156-targeted SQUAMOSA promoter binding-like transcription factors. Plant Cell. 24:3320-3332.

Zhang X, Zhao H, Gao S, Wang WC, Katiyar-Agarwal S, Huang HD, Raikhel N, Jin H (2011) Arabidopsis Argonaute 2 regulates innate immunity via miRNA393(*)-mediated silencing of a Golgi-localized SNARE gene, MEMB12. Mol Cell. 42:356-366.

Zhang X, Zou Z, Zhang J, Zhang Y, Han Q, Hu T, Xu X, Liu H, Li H, Ye Z (2011) Over-expression of sly-miR156a in tomato results in multiple vegetative and reproductive trait alterations and partial phenocopy of the sft mutant. FEBS Lett. 585:435-439.

Zhang Y (2005) miRU: an automated plant miRNA target prediction server. Nucleic Acids Res. 33:W701-704.

Zhu QH, Helliwell CA (2011) Regulation of flowering time and floral patterning by miR172. J Exp Bot. 62:487-495.

Zhu QH, Upadhyaya NM, Gubler F, Helliwell CA (2009) Over-expression of miR172 causes loss of spikelet determinacy and floral organ abnormalities in rice (*Oryza sativa*). BMC Plant Biol. 9:149.